Feasibility of real-time near-infrared indocyanine green fluorescence endoscopy for the evaluation of mucosal head and neck lesions

Florian Schmidt,[1] Andreas Dittberner,[1,2] Sven Koscielny, MD,[1] Iver Petersen, MD,[3] Orlando Guntinas–Lichius, MD[1]*

[1]Department of Otorhinolaryngology, Jena University Hospital, Jena, Germany, [2]Current address: Department of Otorhinolaryngology, Head and Neck Surgery, University of Erlangen–Nuremberg, Erlangen, Germany, [3]Institute of Pathology, Jena University Hospital, Jena, Germany.

ABSTRACT: *Background.* The purpose of this study was to explore the feasibility and potential drawbacks of near-infrared (NIR) endoscopy with indocyanine green (ICG) to examine mucosal head and neck lesions.

Methods. NIR ICG endoscopy was applied to image head and neck cancer epithelium in vivo. The evaluation of the ICG videos was performed off-line independently by 2 evaluators and blinded with respect to final histopathological results from biopsies taken as the gold standard.

Results. Forty percent of the lesions from 55 patients were histologically malignant. ICG positivity showed a sensitivity, specificity, and accuracy to be related to a malignant tumor of 90.5%, 90.9%, and 89.1%, respectively. The kappa index for the interobserver assessment showed a 94.4% agreement for the assessment of the ICG positivity. Side effects of the NIR ICG endoscopy did not arise.

Conclusion. NIR ICG endoscopy in patients with mucosal head and neck lesions was feasible and safe. It might help intraoperatively to differentiate benign from malignant lesions. © 2016 The Authors Head & Neck Published by Wiley Periodicals, Inc. *Head Neck* **39**: 234–240, 2017

KEY WORDS: head and neck cancer, diagnostics, near-infrared endoscopy, fluorescence imaging, indocyanine green, tumor margin

INTRODUCTION

Despite enormous improvement of diagnostic and therapeutic possibilities, 2 of every 3 cases of head and neck cancer are detected in advanced stage and, even after curative treatment, 30% to 50% of patients sustain a locoregional recurrence with worse prognosis.[1] In addition to long periods without symptoms, the difficult access to some head and neck subsites and the field cancerization process are major reasons why it is so difficult to detect head and neck cancer in an early stage as well as to guarantee clear tumor free margins (R0) when approaching a tumor with surgical therapy.[2] Tumor-free margins are a major prognostic factor for local tumor recurrence, which occurs in 7% to 30% of patients with advanced disease.[3] The field cancerization process leads to the fact that the otorhinolaryngologist facing a suspicious lesion in the head and neck region typically is confronted with a combination of inflammatory, dysplastic, and cancerous areas.[4,5] In early-stage cases, it is difficult to differentiate chronic inflammation from early cancer and, in advanced tumors, it is difficult to define the tumor borders clinically, even when using endoscopic or microscopic assistance. Even for benign diseases, it might be very difficult to clearly define the border of the lesion. To date, the clinician can rely only on systematic biopsies and their histopathological grading of the epithelial dysplasia. This is time-consuming, must be performed ex vivo, and has methodological limitations.[6] It is well known that there are other molecular factors indicating genetic altered cells beyond dysplasia that have a major prognostic impact on tumor diagnosis and evaluation of tumor margins.

New optical diagnostics are needed to allow a faster noninvasive (or least less-invasive) differentiation between normal tissue and tumor tissue, between benign and malignant tumor tissue, and between tumor tissue and surrounding inflammation. The development of near-infrared (NIR) optical fluorescent techniques for diagnosis, treatment, and follow-up of head and neck lesions, especially for head and neck cancer, is a growing field that provides real-time information regarding the presence, location, and dimensions of the cancer tissue and/or metastasis through creation of a specific contrast between normal and cancer tissue. This contrast could be the result of tumor-induced morphologic and biochemical alterations that alter optical properties of tissues and lead to tumor-specific autofluorescence. Furthermore, fluorescence can be achieved through

targeting head and neck lesions by fluorescent probes. Indocyanine green (ICG) is such an NIR fluorescent dye. It is approved by the Food and Drug Administration and the European Medicines Agency for determining cardiac output, hepatic function, and liver blood flow, and for ophthalmic angiography, but so far not for head and neck lesions. In the head and neck area, it has been used so far casuistically only as ICG angiography for the monitoring of free flaps or for the evaluation of the relation of larger vessels to skull base tumors.[7,8] It has been applied in paranasal tumors to adapt intra-arterial chemotherapy.[9] Recently, ICG has been introduced as a marker for sentinel node biopsies in patients with head and neck cancer.[10,11] If ICG NIR endoscopy could improve the visualization of the mucosal lesion itself, it has not been evaluated so far. Because of its ability to visualize neoplastic vascularization, it has been shown to support the endoscopic detection of lung metastasis or early gastric cancer as well as the detection of liver metastasis during open abdominal surgery.[12–14]

Therefore, we started a pilot study to explore the feasibility, opportunities, and potential drawbacks of NIR endoscopy with ICG to examine mucosal head and neck lesions.

MATERIALS AND METHODS

Study design and setting

This prospective observational study was performed at the Department of Otorhinolaryngology, Jena University Hospital, Jena, Germany. Approval for the study was obtained through the local institutional review board and informed consent was obtained from all study participants.

Patients and performance of the of near-infrared fluorescence endoscopy

The study cohort consisted of 55 patients with different mucosal head and neck lesions treated between November 2013 and December 2015. Inclusion criteria were age ≥18 years, indication for diagnostic panendoscopy or microlaryngoscopy in general anesthesia and taking biopsies, and written informed consent, including consent for the off-label use of ICG. Exclusion criteria were severe chronic kidney, lung and liver disease, and thyroid autonomy.

Standard panendoscopy or microlaryngoscopy with careful evaluation of the suspected mucosal lesion area and its surrounding tissue was performed. NIR ICG endoscopy was performed before taking the diagnostic biopsies (Figure 1). An NIR-optimized HD camera system (IMAGE1 S NIR/ICG system; Karl Storz, Tuttlingen, Germany) and light source (D-LIGHT P; Karl Storz) were used for NIR endoscopy. This system allows a switchover via a foot-switch between fluorescence and standard white light mode. NIR-optimized telescopes were used (ICG HOPKINS 0° telescope, 5.8 mm diameter, 19 cm length; and ICG HOPKINS 0° telescope, 10 mm diameter, 20 cm length; Karl Storz). Then, ICG (5 mL of 25 mg/15 mL solution = 8.3 mg ICG; Pulsion, Feldkirchen, Germany) was administered intravenously. Before this study, we tested solutions from 25 mg/30 mL to 25 mg/5 mL. The 25 mg/15 mL solution gave the best image contrast. NIR ICG imaging was started directly after application of the contrast

FIGURE 1. Intraoperative setting. Standard panendoscopy was performed, including suspension laryngoscopy. Rigid near-infrared (NIR) with indocyanine green (ICG) endoscopy was performed directly after injection of the ICG. A split screen allowed observation of white light image and fluorescence image at the same time. [Color figure can be viewed at wileyonlinelibrary.com]

agent. The procedure was video-recorded (12 frames/second). Each video had at least duration of 60 seconds. The initial ICG uptake phase was completely recorded in the NIR ICG mode of the imaging system. After the end of this uptake phase, it was switched back and forth several times from the NIR ICG mode to the white light mode of the endoscope before the recording was completed. Finally, standard biopsies were taken from the same areas and preceded for standard histopathology.

Evaluation of the near-infrared indocyanine green videos

The evaluation of the videos was performed off-line. The videos were viewed repeatedly. Additionally, all videos were evaluated in single-frame mode. The images were evaluated independently by 2 evaluators who were blinded with respect to the final histopathological results. The videos were evaluated for 3 parameters: (1) ICG positivity of the head and neck lesion (yes/no) was the first parameter. A lesion was defined as ICG-positive if the lesion showed a fast uptake of ICG within 1 to 2 seconds after ICG injection. Normal mucosal vessels always were ICG-positive. Therefore, it was possible that the lesion itself was ICG-negative but contained ICG-positive vessels. (2) Pooling of ICG was the second parameter (pooling yes/no): some lesions showed a constant ICG labeling throughout the entire video-recording phase and a pooling of ICG within the lesion. (3) The tumor borders were

TABLE 1. Patient characteristics.

Patient characteristics ($n = 55$)	Absolute, no.	Relative, %
Sex		
Female	13	23.6
Male	42	76.4
Localization		
Larynx	32	58.2
Oropharynx	16	29.1
Cavity of the mouth	6	10.9
Hypopharynx	1	1.8
Primary lesion or recurrence		
Primary lesion	45	81.8
Recurrent lesion	10	18.2
Histology		
Squamous cell cancer	18	32.7
Squamous cell hyperplasia	8	14.5
Normal mucosa	7	12.7
Reinke edema	6	10.9
SIN III (severe dysplasia)	3	5.5
Chronic inflammation	3	5.5
Cyst	2	3.6
Polyp	3	5.5
Lymphoma	1	1.8
SIN II (moderate dysplasia)	1	1.8
Papilloma	1	1.8
Papillomatosis	1	1.8
Lymphatic tissue	1	1.8
Malignant tumor		
No	33	60.0
Yes	22	40.0
If malignant ($n = 22$), grading		
2	11	50.0
3	7	31.8
Not applicable	4	18.2
If malignant ($n = 22$), T classification		
T1	1	4.5
T2	8	36.4
T3	8	36.4
T4	1	4.5
Not applicable	4	18.2
	Mean $\pm$ SD	Median, range
Age, y	59 $\pm$ 14	60, 22–80

Abbreviation: SIN, squamous intraepithelial neoplasia.

evaluated as the third parameter. In case of an ICG-positive lesion, the size of the ICG-labeled tumor was compared to the size of the tumor under white light endoscopy (same/larger/smaller).

Statistical analysis

Statistical analyses were performed using IBM SPSS version 23.0 statistical software for Windows (Chicago, IL). If not otherwise indicated, data are reported as mean with SD. The diagnostic accuracy of NIR ICG positivity to prognosticate a malignant tumor was evaluated by a 2-by-2 table and calculation of sensitivity and specificity. Differences concerning the evaluation parameters between 2 subgroups of patients were evaluated with the chi-square test. For all statistical tests, significance was 2-sided and set to $p < .05$ Interobserver variability of the assessment of the NIR ICG findings was analyzed using kappa statistics.

RESULTS

Subjects

Patients' characteristics are summarized in Table 1. Forty-two men and 13 women were included. Mean age was 59 $\pm$ 14 years (range, 22–80 years). The majority of the lesions were localized in the larynx (58%) and the oropharynx (29%). Most cases were primary lesions (82%). The dominant histology was squamous cell cancer or a premalignant squamous intraepithelial neoplasia (SIN) III tumor (33%), followed by benign squamous cell hyperplasia (15%), normal mucosa (13%), and Reinke edema (11%). Overall, 40% were malignant tumors. Complications during the NIR endoscopy were not seen.

### Near-infrared/indocyanine green findings

In general, submucosal vessels were ICG-positive. Benign lesions were ICG-negative and premalignant or malignant tumors (severe dysplasia SIN III and squamous cell cancer) were ICG-positive (Table 2, Figure 2). In ICG-positive tumors, normal ICG-positive vessels were no longer separately identifiable. ICG-positive lesions showed a fast and gradual uptake of the ICG with seconds after the intravenous bolus injection (Figure 3). If the lesion was ICG-positive, it seemed to be of the same size or larger during NIR ICG endoscopy than during white light endoscopy when the lesion was malignant (Table 3). In contrast, ICG size seemed to be smaller than the size in white light endoscopy in benign ICG-positive lesions. Retention of ICG was visible in 21 of 22 ICG-positive lesions; only the benign papilloma showed a strong ICG positivity but no pooling after the ICG uptake phase. The retention of the ICG could be homogeneous or inhomogeneous with an ICG-positive lesion (Figure 2).

TABLE 2. Relation of histopathology to indocyanine green positivity and indocyanine green–positive vessels.

Histopathology	No. of ICG-positive lesions	No. of ICG-negative lesions		Sum, no.
		With ICG-negative vessels	With ICG-positive vessels	
Normal mucosa	0	0	7	7
SIN III (severe dysplasia)	2	1	0	3
Squamous cell cancer	16	1	1	18
Chronic inflammation	1	1	1	3
Lymphoma	1	0	0	1
Cyst	0	0	2	2
Reinke edema	0	0	6	6
SIN II (moderate dysplasia)	0	1	0	1
Polyp	0	0	3	3
Papilloma	1	0	0	1
Papillomatosis	0	0	1	1
Lymphatic tissue	1	0	0	1
Squamous cell hyperplasia	0	8	0	8
Sum	22	12	21	55

Abbreviation: SIN, squamous intraepithelial neoplasia.

FIGURE 2. Endoscopic examples of near-infrared (NIR) with indocyanine green (ICG) finding in different types of mucosal head and neck lesions in the larynx. White light image on the left side (A–E) and corresponding NIR ICG image on the right side (F–J). Normal mucosa (AB) and Reinke edema (BG) only showed ICG positivity in the submucosal vessels. The mucosal hyperplasia on the right anterior vocal cord (CH) was completely ICG-negative, even sparing ICG-positive vessels. The severe dysplasia of the right vocal cord (squamous intraepithelial neoplasia [SIN] III, DI) and the squamous cell cancer of the left anterior vocal cord (T1 glottic cancer, EJ) showed a diffuse ICG positivity and retention of ICG. [Color figure can be viewed at wileyonlinelibrary.com]
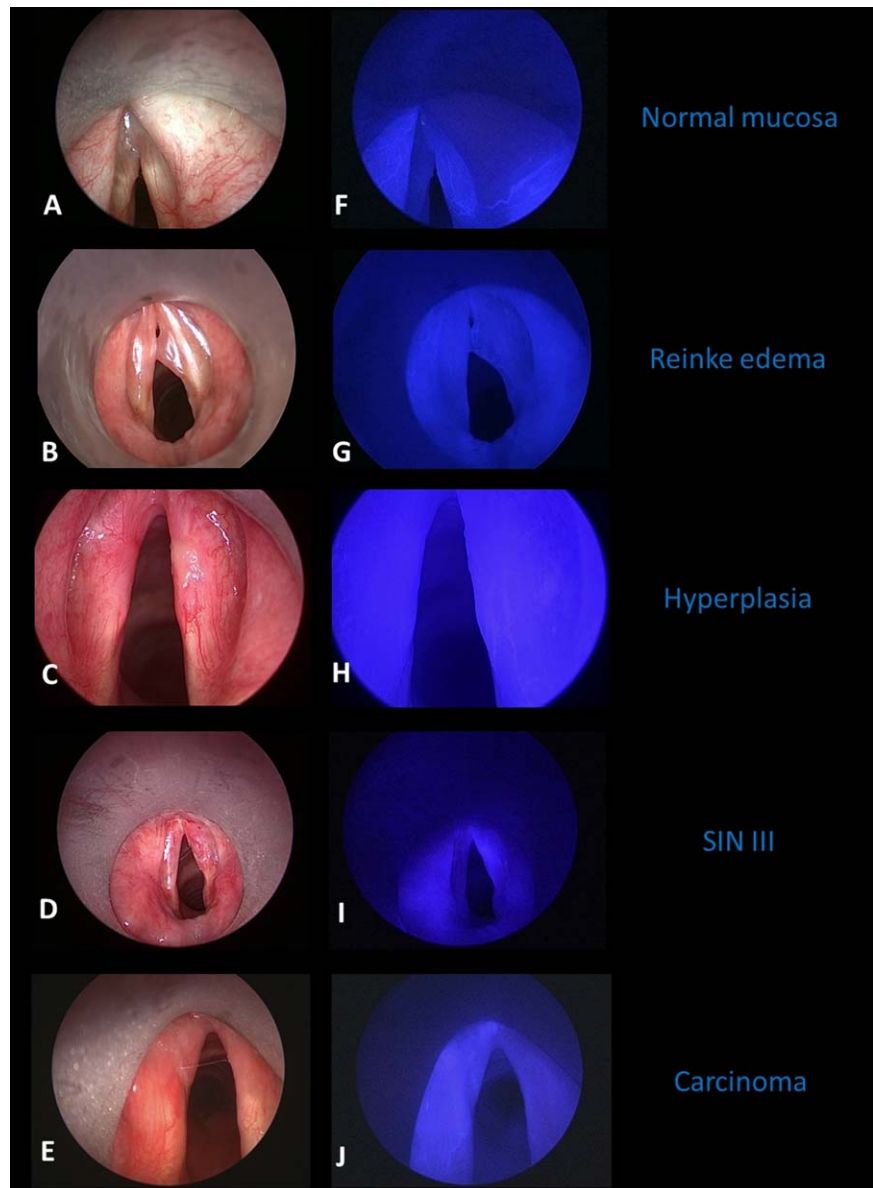
The diagnostic accuracy is shown in Table 4. This resulted in a sensitivity, specificity, and accuracy that ICG positivity was related to a malignant tumor of 90.5%, 90.9%, and 89.1%, respectively.

The kappa index for the interobserver assessment of the NIR ICG finding showed a 94.4%, 79.4%, and 62.5% agreement, respectively, for the assessment of the ICG positivity of the lesion, the size in relation to the white light image, and concerning the retention of ICG within the lesion.

DISCUSSION

In head and neck oncology, NIR fluorescence imaging has so far been introduced for sentinel lymph node mapping and might be a promising alternative to gamma ray-emitting radiotracers for transcutaneous visualization of superficial lymphatic channels and sentinel lymph nodes in the future.[15,16] For direct tumor imaging, it has been used so far in a limited number of studies, mainly in patients with hepatobiliary cancer, colorectal metastases, gastric cancer, or breast cancer.[17–20] To our knowledge, Yokoyama et al[21] were the first to apply NIR ICG endoscopy to visualize the primary head and neck cancer in 5 patients. All 5 patients with oral or oropharyngeal cancers were ICG-positive in their study. The same group recently published a series of 36 patients with advanced paranasal sinus cancer receiving an ICG injection together with intra-arterial chemotherapy. All tumors were ICG-positive by ICG labeling of the tumor-feeding arteries. This was helpful to confirm the target region for intra-arterial chemotherapy, especially in cases in which standard CT angiography was not indicative.[9] Recently, Digonnet et al[22] used NIR ICG imaging primarily to study the fluorescence of negative and negative lymph nodes during neck dissection in 11 patients. Five of these 11 patients
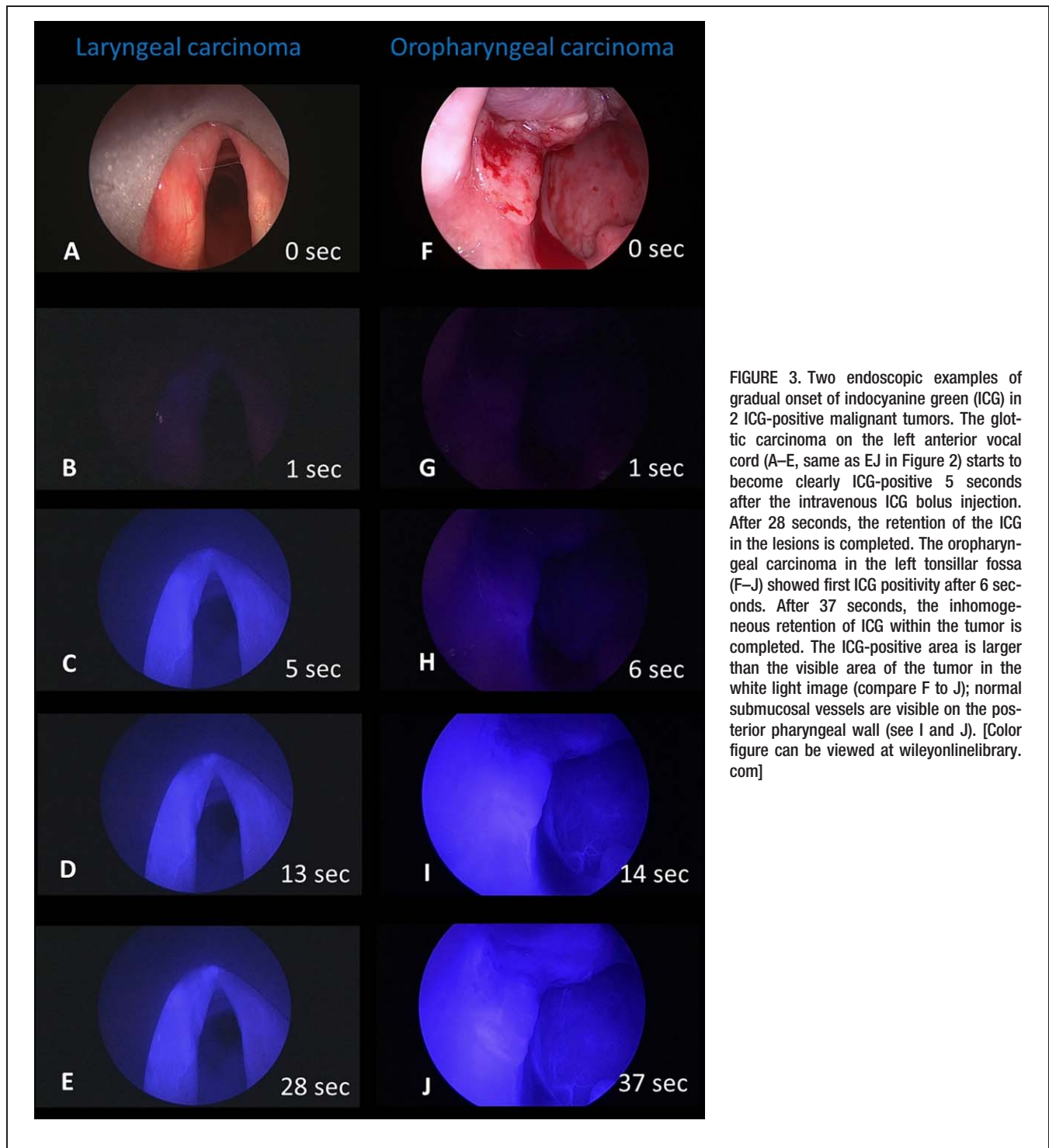
FIGURE 3. Two endoscopic examples of gradual onset of indocyanine green (ICG) in 2 ICG-positive malignant tumors. The glottic carcinoma on the left anterior vocal cord (A–E, same as EJ in Figure 2) starts to become clearly ICG-positive 5 seconds after the intravenous ICG bolus injection. After 28 seconds, the retention of the ICG in the lesions is completed. The oropharyngeal carcinoma in the left tonsillar fossa (F–J) showed first ICG positivity after 6 seconds. After 37 seconds, the inhomogeneous retention of ICG within the tumor is completed. The ICG-positive area is larger than the visible area of the tumor in the white light image (compare F to J); normal submucosal vessels are visible on the posterior pharyngeal wall (see I and J). [Color figure can be viewed at wileyonlinelibrary.com]

also received a resection of the primary tumor. Four of these 5 tumors were ICG-positive (80% vs 89% of the premalignant SIN III tumors or malignant tumors in the present study). The margins were ICG-negative after tumor resection or second resection in 1 case with residual fluorescence. These results and the findings of the present study confirm that ICG positivity is a marker of most head and neck cancers, as it has already been shown for other solid tumors (see above).

No adverse reactions related to the ICG injection occurred in patients with head and neck lesions. It is repeatedly stated in the literature that bolus injections of ≤ 0.25 to 0.5 mg/kg body weight might increase the risk of allergic reactions. However, this statement is actually related to only 1 study.[23] Interestingly, we needed only a fixed dose of 8.3 mg per patients (which would be only 0.12 mg/kg in a patient with 70 kg body weight) to achieve a fast visualization within seconds to minutes,

TABLE 3. Relation of histopathology to size of the indocyanine green–positive lesion compared to the size during white light endoscopy.

Histopathology	Same	Larger	Smaller	Sum
SIN III (severe dysplasia)	0	2	0	2
Squamous cell cancer	8	7	1	16
Chronic inflammation	1	0	0	1
Lymphoma	0	0	1	1
Papilloma	0	0	1	1
Lymphatic tissue	0	0	1	1
Sum	9	9	4	22

Abbreviation: SIN, squamous intraepithelial neoplasia.

whereas others report a best visualization with 0.5 mg/kg ICG within 60 to 120 minutes.[21] We can only speculate that our imaging system might be better able to detect the fluorescence than other systems.

ICG is a nontargeted probe and itself not cancer-specific. It binds to plasma proteins, remains within the vascular system, and does not diffuse into the interstitial space under physiological conditions.[15] It is proposed that the peritumoral vascular hyperpermeability is one reason for the tumor fluorescence.[16] This might be the reason why tissue with strong vascularization, like the lymphatic tissue of the tonsil or a benign papilloma, or hyperpermeability because of inflammation, also could show (false) ICG positivity. Furthermore, tumor neovascularization is characterized by newly formed and more porous blood vessels, leading to passive accumulation of ICG in tumor tissue.[15] This results in retention and pooling of ICG within the malignant tumor, as it could be seen even in a premalignant lesion and in early glottic cancer (SIN III lesion or T1 glottic cancer, respectively) in the present study or as a characteristic feature of early glottic cancer.[17,24] Interestingly, the ICG signal not only helped to differentiate between benign and malignant lesions, but also to differentiate different types of benign lesions. The normal submucosal vessels system in the head and neck mucosa is always ICG-positive. In case of benign squamous cell hyperplasia, the region of the lesion was spared from these vessels. It might be that the hyperplasia covered the fluorescence of the vessels in a deeper layer. Future studies should show how thick such a hyperplasia must be to cover ICG-positive vessels. This is important because this factor could be important in (false) ICG-negative malignant tumors. Furthermore, at the moment, targeted fluorescent dyes in the NIR range are being

TABLE 4. Diagnostic accuracy of indocyanine green positivity of malignant tumors ($n = 55$).*

	No. of ICG-negative	No. of ICG-positive	p value
Benign process, no.	30	3	< .0001
Malignant tumors, no.*	3	19	
Sum	33	22	

Abbreviation: ICG, indocyanine green.
* Including premalignant squamous intraepithelial neoplasia (SIN III) lesions.

introduced into clinical trials, which might replace nontargeted ones in the near future.[25,26] This will further improve the accuracy of the technology.

Beyond ICG positivity, the demarcation of the tumor borders is of interest in respect of image-guided surgery.[27] In the present study, the tumor borders appeared to be larger under ICG than under white light endoscopy, but the true histological borders were not correlated to the endoscopic appearance. If ICG-guided surgery could lead to clearer tumor margins and better outcome, it has to be shown in future studies with histological correlations. In any case, it has been shown already that a repetition of the NIR ICG endoscopy directly after tumor resection can help to obtain clear margins because the wound bed should be ICG-negative after resection.[22]

The advantage of NIR ICG imaging is that several endoscopy systems as well as ICG are licensed and on the market. The NIR light does not alter the vision of the surgeon and it is easy to switch between white light and ICG image. Furthermore, the signal-to-background ratio is impressive because of very low autofluorescence.[15] In contrast, a dense submucosal vascular network, like in the tonsils, might make it more difficult to demarcate a melanoma against the background. The good tissue penetration of about 5 to 10 mm is an advantage to other optical imaging techniques (for instance, autofluorescence, confocal laser endomicroscopy, or optical coherence tomography), but, of course, still not enough to get an overview of larger tumors (>T1).[28]

The diagnostic accuracy, sensitivity, and specificity to predict a malignant tumor by ICG positivity was satisfactory for such a first feasibility study. One should not forget that the evaluation was performed offline by watching the videos repeatedly and in single-frame modus. Furthermore, it should be stressed that the contrast between "ICG-positive" and "ICG-negative" regions was only subjectively evaluated, so the method lacks any objectivity (apart from the interobserver evaluation). Especially with regard to a possible application during a resection of tumors, where blood, tissue debris, and coagulation artifacts might reduce the contrast even further, a high contrast would be mandatory. It would be worthwhile to develop automated image analysis methods for ICG images as it has also ready been introduced for confocal laser endomicroscopy images.[29] For optical image-guided surgery, it would be helpful to develop tools to overlay ICG image and white light image.[30] Finally, the approval of tumor-specific NIR probes or the conjunction of tumor-specific antibodies with unspecific NIR probes will be the most important step to develop intraoperative image-guided cancer surgery.[31]

CONCLUSIONS

NIR ICG endoscopy was feasible in 55 patients with different mucosal head and neck lesions. Complications were not seen. For a first feasibility study, the diagnostic accuracy analysis to predict a malignant tumor by offline evaluation of the ICG videos for ICG positivity of the tumors was satisfactory. The analysis showed a sensitivity, specificity, and accuracy that ICG positivity of the tumor was related to a malignant tumor of 90.5%, 90.9%, and 89.1%, respectively. This has to be confirmed in

larger confirmatory studies, including tumors that are more advanced and especially in relation to the correlation between ICG tumor margins and histological tumor margins.

REFERENCES

1. Argiris A, Karamouzis MV, Raben D, Ferris RL. Head and neck cancer. *Lancet* 2008;371:1695–1709.
2. Braakhuis BJ, Brakenhoff RH, Leemans CR. Second field tumors: a new opportunity for cancer prevention? *Oncologist* 2005;10:493–500.
3. Anderson CR, Sisson K, Moncrieff M. A meta-analysis of margin size and local recurrence in oral squamous cell carcinoma. *Oral Oncol* 2015;51: 464–469.
4. Slaughter DP, Southwick HW, Smejkal W. Field cancerization in oral stratified squamous epithelium; clinical implications of multicentric origin. *Cancer* 1953;6:963–968.
5. Leemans CR, Braakhuis BJ, Brakenhoff RH. The molecular biology of head and neck cancer. *Nat Rev Cancer* 2011;11:9–22.
6. Hinni ML, Ferlito A, Brandwein–Gensler MS, et al. Surgical margins in head and neck cancer: a contemporary review. *Head Neck* 2013;35:1362–1370.
7. Betz CS, Zhorzel S, Schachenmayr H, et al. Endoscopic assessment of free flap perfusion in the upper aerodigestive tract using indocyanine green: a pilot study. *J Plast Reconstr Aesthet Surg* 2013;66:667–674.
8. Inoue A, Ohnishi T, Kohno S, et al. Usefulness of an image fusion model using three-dimensional CT and MRI with indocyanine green fluorescence endoscopy as a multimodal assistant system in endoscopic transsphenoidal surgery. *Int J Endocrinol* 2015;2015:694273.
9. Yokoyama J, Ohba S, Fujimaki M, Kojima M, Suzuki M, Ikeda K. Significant improvement in superselective intra-arterial chemotherapy for advanced paranasal sinus cancer by using indocyanine green fluorescence. *Eur Arch Otorhinolaryngol* 2014;271:2795–2801.
10. Nakamura T, Kogashiwa Y, Nagafuji H, Yamauchi K, Kohno N. Validity of sentinel lymph node biopsy by ICG fluorescence for early head and neck cancer. *Anticancer Res* 2015;35:1669–1674.
11. Christensen A, Juhl K, Charabi B, et al. Feasibility of real-time near-infrared fluorescence tracer imaging in sentinel node biopsy for oral cavity cancer patients. *Ann Surg Oncol* 2016;23:565–572.
12. Ishihara R. Infrared endoscopy in the diagnosis and treatment of early gastric cancer. *Endoscopy* 2010;42:672–676.
13. van der Vorst JR, Schaafsma BE, Hutteman M, et al. Near-infrared fluorescence-guided resection of colorectal liver metastases. *Cancer* 2013; 119:3411–3418.
14. Anayama T, Qiu J, Chan H, et al. Localization of pulmonary nodules using navigation bronchoscope and a near-infrared fluorescence thoracoscope. *Ann Thorac Surg* 2015;99:224–230.
15. Schaafsma BE, Mieog JS, Hutteman M, et al. The clinical use of indocyanine green as a near-infrared fluorescent contrast agent for image-guided oncologic surgery. *J Surg Oncol* 2011;104:323–332.
16. Zelken JA, Tufaro AP. Current trends and emerging future of indocyanine green usage in surgery and oncology: an update. *Ann Surg Oncol* 2015;22 Suppl 3:S1271–S1283.
17. Mataki N, Nagao S, Kawaguchi A, et al. Clinical usefulness of a new infrared videoendoscope system for diagnosis of early stage gastric cancer. *Gastrointest Endosc* 2003;57:336–342.
18. Gotoh K, Yamada T, Ishikawa O, et al. A novel image-guided surgery of hepatocellular carcinoma by indocyanine green fluorescence imaging navigation. *J Surg Oncol* 2009;100:75–79.
19. Watanabe M, Tsunoda A, Narita K, Kusano M, Miwa M. Colonic tattooing using fluorescence imaging with light-emitting diode-activated indocyanine green: a feasibility study. *Surg Today* 2009;39:214–218.
20. Tummers QR, Verbeek FP, Schaafsma BE, et al. Real-time intraoperative detection of breast cancer using near-infrared fluorescence imaging and Methylene Blue. *Eur J Surg Oncol* 2014;40:850–858.
21. Yokoyama J, Fujimaki M, Ohba S, et al. A feasibility study of NIR fluorescent image-guided surgery in head and neck cancer based on the assessment of optimum surgical time as revealed through dynamic imaging. *Onco Targets Ther* 2013;6:325–330.
22. Digonnet A, van Kerckhove S, Moreau M, et al. Near infrared fluorescent imaging after intravenous injection of indocyanine green during neck dissection in patients with head and neck cancer: a feasibility study. *Head Neck* 2016;38 Suppl 1:E1833–E1837.
23. Speich R, Saesseli B, Hoffmann U, Neftel KA, Reichen J. Anaphylactoid reactions after indocyanine-green administration. *Ann Intern Med* 1988; 109:345–346.
24. Iseki K, Tatsuta M, Iishi H, Sakai N, Yano H, Ishiguro S. Effectiveness of the near-infrared electronic endoscope for diagnosis of the depth of involvement of gastric cancers. *Gastrointest Endosc* 2000;52:755–762.
25. van Driel PB, van der Vorst JR, Verbeek FP, et al. Intraoperative fluorescence delineation of head and neck cancer with a fluorescent anti-epidermal growth factor receptor nanobody. *Int J Cancer* 2014;134:2663–2673.
26. Fidel J, Kennedy KC, Dernell WS, et al. Preclinical validation of the utility of BLZ-100 in providing fluorescence contrast for imaging spontaneous solid tumors. *Cancer Res* 2015;75:4283–4291.
27. Keereweer S, Van Driel PB, Snoeks TJ, et al. Optical image-guided cancer surgery: challenges and limitations. *Clin Cancer Res* 2013;19:3745–3754.
28. Rosenthal EL, Warram JM, Bland KI, Zinn KR. The status of contemporary image-guided modalities in oncologic surgery. *Ann Surg* 2015;261:46–55.
29. Dittberner A, Rodner E, Ortmann W, et al. Automated analysis of confocal laser endomicroscopy images to detect head and neck cancer. *Head Neck* 2016;38 Suppl 1:E1419–E1426.
30. Elliott JT, Dsouza AV, Davis SC, et al. Review of fluorescence guided surgery visualization and overlay techniques. *Biomed Opt Express* 2015;6: 3765–3782.
31. Chi C, Du Y, Ye J, et al. Intraoperative imaging-guided cancer surgery: from current fluorescence molecular imaging methods to future multimodality imaging technology. *Theranostics* 2014;4:1072–1084.